Modelling of lake mixing induced by air-bubble plumes and the effects on evaporation

Modelling of lake mixing induced by air-bubble plumes and the effects on evaporation

Fernanda Helfer[a,*], Hong Zhang[a], Charles Lemckert[a]

[a]Griffith School of Engineering, Griffith University, Gold Coast, QLD, Australia

*Corresponding author address: Building G09, Room 1.02, Griffith School of Engineering, Gold Coast Campus, Griffith University, QLD 4222. Tel.: +61 (0)7 5552 7608; Fax: +61 (0)7 5552 8065. E-mail: f.helfer@griffith.edu.au

Abstract

One of the main concerns regarding water storage in Australia, and other semi-arid countries, is the high rate of evaporation that inevitably leads to significant water loss. In this paper, the use of air-bubble plume systems to reduce evaporation from large reservoirs is assessed. A destratification system was designed for a large dam based on its depth and stratification strength with the intention of destratifying the reservoir in a short time period. The model DYRESM was then used to simulate the water dynamics under destratification conditions. Different strategies for the operation of the aeration system were assessed, from 10-day operation periods at times of high evaporation rates to continuous operation over longer time spans. The modelled water column temperatures and evaporation rates were analysed and it was found that artificial destratification was only effective in reducing evaporation in spring. In summer, heat is added to the water at a rapid rate, and artificial destratification only helps reduce evaporation in the initial days of operation. The effect of artificial destratification in reducing evaporation in autumn depends on the operation of the system during summer. If operated in summer, the rates of evaporation in autumn will increase due to the additional heat added to the water during the summer. In winter, overturn takes place and artificial destratification has no influence on water temperatures and evaporation. It was concluded that aeration by air-bubble plumes would only be effective in

reducing evaporation if the hypolimnetic water does not become warm when mixing takes place. This is an ideal situation, but is unlikely to happen in practice.

Keywords: evaporation; aeration; destratification; water temperature, DYRESM

1. Introduction

In hot, dry areas, the loss of water from open water reservoirs through evaporation can be significant. In countries where water is becoming scarce – as a result of population growth, industrial development, increase of living standards and irrigated agriculture – minimizing evaporation losses is becoming more important. Gökbulak and Özhan (2006) estimated that annual evaporation from lakes and dams in Turkey is greater than the amount of water withdrawn for domestic and industrial purposes across the country. In the semi-arid region of south-eastern Spain, evaporation from reservoirs was found to be equivalent to 27% of the urban demand (Martínez Alvarez et al., 2008). In northern New South Wales and Queensland, Australia, annual evaporation loss was estimated to be as high as 40% of the total storage capacity (Craig et al., 2005). These examples suggest that important water savings could be achieved by reducing evaporation from open water storages in arid and semi-arid countries.

Australia is estimated to have around 92,000-hm^3 capacity for surface-water storage, comprising 84,000 hm^3 in large dams (Australian Bureau of Statistics, 2006) and 8,000 hm^3 in farm dams (National Land & Water Resources Audit, 2001). In Queensland, the storage capacity is 11,000 hm^3 with Wivenhoe Dam (Figure 1) alone being responsible for 2,600 hm^3 (SEQWater, 2009). Approximately 1,160 hm^3 of the stored water in Wivenhoe is used to supply water to the south-east Queensland region and about 160 hm^3 evaporates each year, which would be sufficient to supply around 1.5 million people during a year.

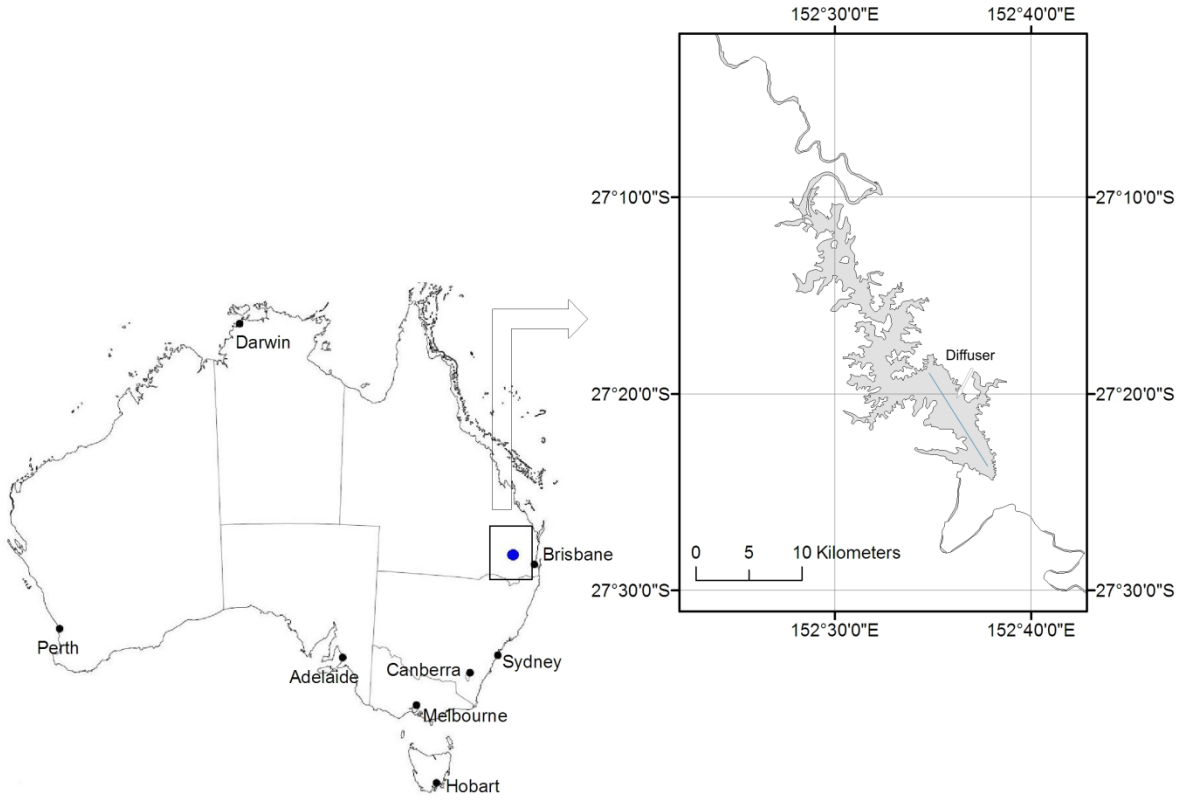

Figure 1. Location of Wivenhoe Dam in Australia and the hypothetical location of a destratification system

Recent studies have investigated the application of different mechanisms to reduce evaporation from large dams, such as Wivenhoe, in Queensland. McJannet et al. (2008a) studied the effects of modifying the dam's surface area to volume ratios and concluded that this would not yield significant evaporation reductions. The same authors also studied the use of monolayers and found a possible reduction in evaporation of 10% - an important saving - although with questionable effects upon the water quality (McJannet et al., 2008b). Yao et al. (2010) investigated the effectiveness of suspended and floating covers in reducing evaporation from Wivenhoe Dam and the results showed an impressive reduction in evaporation of 76% for suspended covers and 68% for floating covers. However, the size of Wivenhoe Dam, the risk to dam wall integrity during flood events, and the likely (but unknown) adverse impact on water quality immediately eliminates the possibility of covering the whole dam and a smaller area of application would need to be considered. Helfer et al.

(2009) investigated the use of windbreaks as a mechanism to reduce evaporation from large dams and found a minor reduction of only 5.6% in evaporation rates.

One other technique that could be used to reduce evaporation from open waters is lake aeration (or destratification) by bubble plumes. Air-bubble plumes have been suggested by Koberg and Ford (1965) and Hughes et al. (1975) as a mechanism for evaporation control and tested recently by van Dijk and van Vuuren (2009), Helfer et al. (2010) and Helfer et al. (2011a) but with no success for small, shallow dams.

Artificial destratification has long been reported in the literature as a common technique to break down or impede the formation of thermal stratification in lakes to improve water quality (eg, Scott and Foley, 1921; Cooley and Harris, 1954; Fast, 1968; Tolland, 1977; Burns and Powling, 1981; Schladow and Fisher, 1995; Imteaz et al., 2003; Amano, 2004; Imteaz et al., 2009). Thermal stratification generally occurs in large, deep water bodies at mid and high latitudes, in zones with four well defined seasons. The process starts in mid spring when air temperatures are rising. During early spring, these water bodies show an evenly distributed temperature profile as a result of the cooling process which takes place in winter. As the air temperatures start to rise, the rate of surface heating begins to exceed the rate of transfer of heat to deeper water layers. As a result, the surface of the water body becomes warmer than the bottom and a zone of generally rapid decrease in temperature, called the thermocline, develops just below the surface layer. This thermal stratification impedes the hypolimnetic water from having contact with the atmosphere and re-oxygenating. Consequently, the stagnated hypolimnetic water can become anoxic, which affects the aquatic life and gives rise to the release of nutrients and metal compounds from the sediments at the bottom of the lake. This eutrophication greatly affects the quality of the water for consumption (Mortimer, 1941). The difficulty of the warm surface water to mix with cold bottom water is also an indication of greater evaporation rates (Eichinger et al., 2003; Rosenberry et al., 2007).

A number of reviews have outlined the methods used for destratifying lakes artificially (Tolland, 1977; Henderson-Sellers, 1982), which include mechanical stirrers, water pumps and air-bubble plume systems. For reservoirs, the most common destratification device is an air-bubble plume system (Imberger and Patterson, 1990), which consists of a perforated pipe at the bottom of the lake, through which compressed air is pumped. As the air-bubbles rise to the surface they carry the hypolimnetic cold fluid with them. This colder water is ejected from the plume when the density of the air-water mixture is approximately equal to the ambient density or when the surface is reached. Once ejected, and being relatively heavy in comparison to the ambient water, the cold water drops, and mixing occurs, reducing thermal stratification. Should the detrainment process occur before the surface is reached, the bubbles continue to rise and further water is entrained, forming a new plume and a later detrainment at a higher level. This process may be repeated several times until the air-bubbles reach the surface. The success of the mixing will depend basically on the plume being sufficiently buoyant to overcome the strength of the stratification. The efficiency will thus depend on the air-flow rate injected into the water and the stratification strength (McDougall, 1978; Schladow, 1992; Asaeda and Imberger, 1993).

The potential of destratification by bubble plumes in reducing evaporation is related to the change in surface water temperature brought about by the mixing device. The cold bottom water lifted up by the air mixes with warm water, reducing the temperature, and consequently, evaporation rates. Given this principle, the most important condition to achieve significant evaporation suppression from lakes is the existence of sufficient water depth (greater than ±18 m) to produce a marked natural thermocline and provide a relatively large volume of cold water for mixing (Hughes et al., 1975).

In this study, the use of destratification by air-bubble plumes to reduce evaporation from large dams is investigated using modelling techniques. A special focus is given to the

seasonal effectiveness of artificial destratification by analysing the performance of the technique over a period of 3 years. Different designs of air bubble plume destratification systems and operating strategies are tested in order to find a combination that maximizes the reduction in evaporation.

2. Air-Bubble Plume Model and Design

In the past, the design methodologies for destratification systems were based on empirical approaches, such as those of Lorenzen and Fast (1977) and Davis (1980) which neglected the fact that bubble-plumes have different behaviour under different conditions. An advance in understanding plume behaviour came from McDougall (1978), who developed a model to describe the rise, detrainment and reformation of a bubble plume in stratified environments. The model is based on the integration of equations of conservation of mass, momentum and buoyancy for a single-phase buoyant plume but maintaining the buoyancy effects of stratification, bubble slip and bubble expansion. McDougall (1978) found that the behaviour of a bubble plume is controlled by two main non-dimensional parameters, M_M and C_M:

$$M_M = \frac{Q_0 p_a \left(\lambda^2 + 1\right)}{4\pi\alpha^2 \rho_r H^2 u_B^3} \tag{1}$$

$$C_M = \left(\frac{N^3 H^4}{g Q_0}\right)\left(\frac{H}{h_a}\right) \tag{2}$$

where Q_0 is the air-flow rate injected into the water at atmospheric pressure ($m^3\ s^{-1}$), p_a is the atmospheric pressure (Pa), H is the total pressure head at the diffuser level including atmospheric pressure (m), h_a is the equivalent head of water (≈10.2 m), N is the buoyancy frequency (s^{-1}), defined as $N = [-(g/\rho_r)d\rho_0/dz]^{1/2}$, where g is the gravity ($m\ s^{-2}$), ρ_r is the reference liquid density ($kg\ m^{-3}$) and $d\rho_0/dz$ is the density gradient ($kg\ m^{-3}\ m^{-1}$). The velocity

scale, u_B, is defined as $u_s(\lambda^2+1)$, where u_s is the slip velocity of the bubbles relative to the liquid in the plume (=0.3 m s^{-1}), λ is the dispersion term, taken to be 0.3 (dimensionless) and α is the entrainment coefficient (dimensionless), taken to be 0.083 (Milgram, 1983). The parameter M_M represents the air source strength compared to the pressure head and C_M represents the effect of the stratification compared to the strength of the source. A high value of C_M represents a case where stratification is strong compared to the source strength. On the other hand, a low value of C_M represents a high source strength compared to the level of stratification and favours the plume reaching the surface without any internal detrainments. Aeration systems with same values of M_M and C_M are expected to promote the same mixing patterns in the water.

In order to dismantle a thermal stratification structure, high airflow rates will be required if the stratification is strong, and low airflow rates will be required if the stratification is weak. If the air-flow rate is too low compared to the stratification strength, it will make the plume detrain water before reaching the surface, sometimes even before reaching the thermocline. However, if the plume is to be effective, it must penetrate this region. If the flow rate is too high and stratification is weak, the plume will only detrain at the surface and energy will be wasted. Physically, the first case will occur whenever the additional buoyancy imparted by the bubbles is insufficient to counter the negative buoyancy of the hypolimnion water. The second case will occur whenever the difference between mean plume density and ambient density remains positive through the entire water column. These two considerations indicate that an optimum airflow rate that provides complete disintegration of the thermal structure with minimum waste of energy may be found, such that the difference between plume and environment densities (density anomaly) just becomes zero at the surface (Patterson and Imberger, 1989).

This effect can be demonstrated by analysing the efficiency of the process, given by the relation between the change in stored potential energy in time (ΔP) and the net energy input by the aerator during this time, given by ($\rho_r Q_0 hg$). Therefore, from the discussion above, for a fixed stratification value of magnitude N, a value of Q_0 may be found which maximizes the destratification efficiency.

A design methodology based on this theory has been suggested by Schladow (1993) and Asaeda and Imberger (1993). An outline of the application of these methodologies is presented by Lemckert et al. (1993). The design methodologies consist of finding the air-flow rate per diffuser and the number of ports required to dismantle efficiently a given stratification (represented by the equivalent linear profile, N_E suggested by Lemckert and Imberger, 1993) and depth.

3. Dynamic Reservoir Simulation Model (DYRESM)

In this study, the one-dimensional processed-based model DYRESM (Imberger and Patterson, 1981) was applied to model lake mixing dynamics under artificial destratification conditions and predict water temperatures and evaporation rates. This model takes lake morphometry (represented by a depth-area relationship of the lake), daily or sub-daily meteorological forcing data (solar radiation, wind, air temperature and air humidity), volume of inflows and outflows, and then produces daily outputs for water temperature, salinity and density. In DYRESM, the reservoir is represented by a series of horizontal layers of uniform properties. These layers are dynamic in thickness due to changes in volume produced by mixing, inflows, outflows, rainfall and evaporation.

The five basic processes modelled by DYRESM are: surface fluxes of heat, mass and momentum; mixed layer dynamics; vertical diffusion in the hypolimnion; inflows; and outflows. The model was later updated to include the mixing by destratification systems such

as bubble plume diffusers and surface mechanical mixers with draft tubes (Patterson and Imberger, 1989).

Within the scope of this paper, the processes of surface fluxes, surface mixed layer dynamics and artificial mixing by air-bubble plume assume more importance. The evolution of the model and the other routines are fully described in the literature (Imberger et al., 1978; Spigel and Imberger, 1980; Imberger and Patterson, 1981; Patterson et al., 1984; Hocking et al., 1988; Patterson and Imberger, 1989).

3.1. Surface fluxes

The surface heat, mass and momentum exchanges comprise the primary mechanisms for heating, mixing and stratifying a water body in DYRESM. The surface energy fluxes are computed using bulk aerodynamic formulae. The fluxes of long-wave radiation, sensible heat and evaporation are assumed to operate on only the surface layer. Short-wave radiation heat input, on the other hand, decays through the water column according to the Beer-Lambert law. For the evaporative heat flux, the bulk aerodynamic formula used is:

$$Q_E = \rho_a \lambda C_E U (q_a - q_s) \quad (3)$$

where Q_E is the latent heat flux due to evaporation (W m^{-2}), ρ_a is the air density (=1.2 kg m^{-3}), λ is the latent heat of evaporation (=2.453E+6 J Kg^{-1}), C_E is the latent heat transfer coefficient (a parameter that is dependent on the water body characteristics), U is the wind speed at the reference height of 10 m (m s^{-1}), q_a is the specific humidity in the air (mass of water vapour per unit mass of moist air) and q_s is the specific humidity at saturation pressure, which is a function of the surface water temperature (Brutsaert, 1982).

The surface mass exchanges include rainfall (input) and evaporation (output). The mass of the evaporated water during a given time interval is calculated as:

$$M_N = -\frac{Q_E A_N}{\lambda} \tag{4}$$

where M_N is the evaporating mass (kg s^{-1}) from the surface layer with area A_N (m^{-2}).

3.2. Mixed Layer Dynamics

The formation and deepening of the epilimnion is computed by evaluating the turbulent kinetic energy budget in the surface mixed layer and the required potential energy for mixing this layer and the adjacent layer. A full description of the process of mixing is given by Yeates and Imberger (2003).

The turbulent kinetic energy budget is composed of three main processes: convective overturn (where energy is released from the decrease in potential energy resulting from dense water falling to a lower level), stirring (where energy from the wind stress is applied to the surface layer), and shear (where kinetic energy is transferred from upper to the lower layers in the water column). The total available energy is compared with the potential energy required to deepen the mixed layer by one computational layer. If the energy available is greater than the energy required, deepening of the surface mixed layer takes place and the available energy is decremented by this energy required for mixing. The process is repeated until there is no remaining energy to continue the deepening process.

Whenever layers are mixed together, the layer properties are redistributed according to the conservation laws. This is valid for temperature, salt, energy and momentum:

$$C_{new} = \frac{C_i M_i + C_{i+1} M_{i+1}}{M_i + M_{i+1}} \quad (5)$$

where the subscripts refer to layer indices and *C* is the property being conserved (energy, salt or momentum) and *M* is the layer mass. For conservation of temperature, the above assumes the specific heat to be constant.

3.3. Mixing by Air-Bubble Plumes

An algorithm to model the mixing of the water by artificial air-bubble plume systems was incorporated into DYRESM and successfully validated with field data in previous studies, such as Patterson and Imberger (1989), Imteaz and Asaeda (2000) and Lewis et al. (2001). The mixing model is based on the single plume model described by McDougall (1978). The model uses the same layer discretisation used in the main model, with the bubble plume entraining water from each layer as it passes through them as a result of the integration of equations for mass, momentum, and buoyancy. The stratification through which the plume rises is not confined to being linear, but rather it is the simulated density profile from the previous time-step.

The plume density is the density of the mixture of air and water. As it rises, the effective buoyancy anomaly decreases as entrainment lowers the plume density at the same time that the ambient density decreases (if the water is stratified). Eventually, the buoyancy anomaly becomes zero, at which height the plume is ejected horizontally into the reservoir, and the plume restarted. The detrained water is immediately routed to its neutrally buoyant level, without entrainment.

The inputs for this destratification part in DYRESM include the number and depth of diffusers operating in the lake, the number of holes on each diffuser and the total daily air-flow rate per diffuser.

4. Model Set-Up and Verification

Wivenhoe Dam (see Figure 1) is a large dam built on the Brisbane River with its main purposes being flood mitigation and the supply of potable water to the south-east Queensland region, Australia. At full capacity, this dam has a volume of 1,160 hm^3 and a surface area of 107 km^2, with a maximum depth of 40 metres. The elevation-area-volume curves are presented in Figure 2.

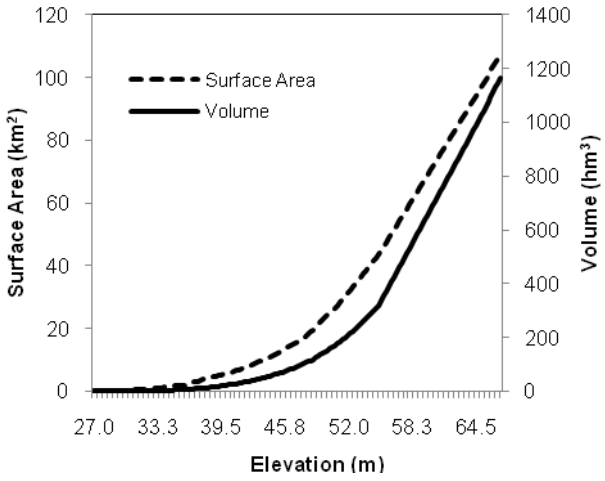

Figure 2. Elevation-area-volume curve for Wivenhoe Dam

In this study, vertical mixing processes were assumed to be more important than horizontal advective processes, such as inflows and outflows, in determining the vertical temperature distribution in Wivenhoe Dam. In large reservoirs such as this, where inflows and outflows have only localized effects on water temperature, these flows can be neglected when predicting the temperature in the central portion of the lake (Ivey and Patterson, 1984). Moreover, other studies on the temperature dynamics of Wivenhoe Dam (eg, Yao, 2008)

have found good agreement between modelled and measured temperatures without considering inflows and outflows.

4.1. Model Verification for Water Temperature

Field measurements of Wivenhoe Dam's water temperature were obtained from South East Queensland Water and used to verify DYRESM. The year 2007 was chosen due to the availability of reliable temperature records. The temperatures were measured from the surface to 21 metres below the surface at 3-m intervals every 7 days.

The light extinction coefficient, *albedo* and bulk transfer coefficient were applied to calibrate DYRESM. The light extinction coefficient influences the thermodynamics of the lake through the varying water column heat absorption (Kling, 1988), but no measured data for this parameter was available for Wivenhoe Dam. The light extinction coefficient is a relatively uncertain factor. It is usually not measured directly but calculated using empirical formulae relying on other parameters like secchi-disk depth or phytoplankton concentrations (Hornung, 2002). Therefore, a mean annual, depth averaged value had to be assumed for the simulations. We tested different values in DYRESM, from 0.3 to 2.0 (Tanentzap, 2006; Kirk, 2003) and compared the simulated water temperature to the measured temperature. The best adjustment was achieved for a value of 1.5 m^{-1}. This relatively high value seems justified, since the lake was modelled at a relatively shallow water depth, which resulted in higher turbidity than at full capacity, giving a high value for the attenuation coefficient (Oliver et al., 2000).

The *albedo* of the water is another site specific parameter. It is the ratio of the global short-wave reflected radiative flux and the flux of the corresponding incident radiation. Generally, the *albedo* is a rather complex function of the angle of the sun, the relative proportion of direct and diffuse radiation (which is a function of the cloud cover fraction) and the surface

roughness (which is a function of wind velocity and the water colour) (Hornung, 2002). For calculations of daily radiation totals, it is common practice to use a mean value of the *albedo* (eg, Brutsaert, 2005). In this study, three mean values of *albedo* were tested, 0.06, 0.08 and 0.12, following Tanentzap et al. (2007). When comparing modelled and measured water temperatures, the best adjustment was obtained with a mean annual *albedo* set equal to 0.12.

The bulk transfer coefficient C_E incorporates the variability induced by influences such as the stability of the meteorological boundary layer over the water surface, the fetch length, wind duration and water depth (Fisher et al., 1979). In DYRESM, this value is taken as a constant unless the user invokes the algorithm for non-neutral atmospheric stability, in which case the value of C_E is found from an iterative procedure as outlined in Hicks (1972). In the current study, neutral atmospheric stability was assumed (following similar studies - eg, Hornung, 2002; Gal et al., 2003; Yeates and Imberger, 2003; Tanentzap, 2006). As local data was limited, an indirect calibration was used - comparing modelled water temperatures with measured water temperatures for values of C_E ranging from 0.8×10^{-3} to 1.6×10^{-3} (Fisher et al., 1979). The value of 1.4×10^{-3} yielded the best agreement between model and field data and it is in accordance with the value suggested for remote land-based meteorological stations by the TVA report (1972) and with the mean values of C_E presented by Hicks (1972) for water bodies of different sizes.

Figures 3 and 4 show that the calibrated model reproduced very well the observed seasonal variation as well as the magnitude of the water temperatures. The coefficient of determination (R^2) for the adjustment, considering 52 days of available measured data, was 0.92, the root-mean-square error (RMSE) was 0.9^{o}C and the mean bias error (MBE) was -2.0%.

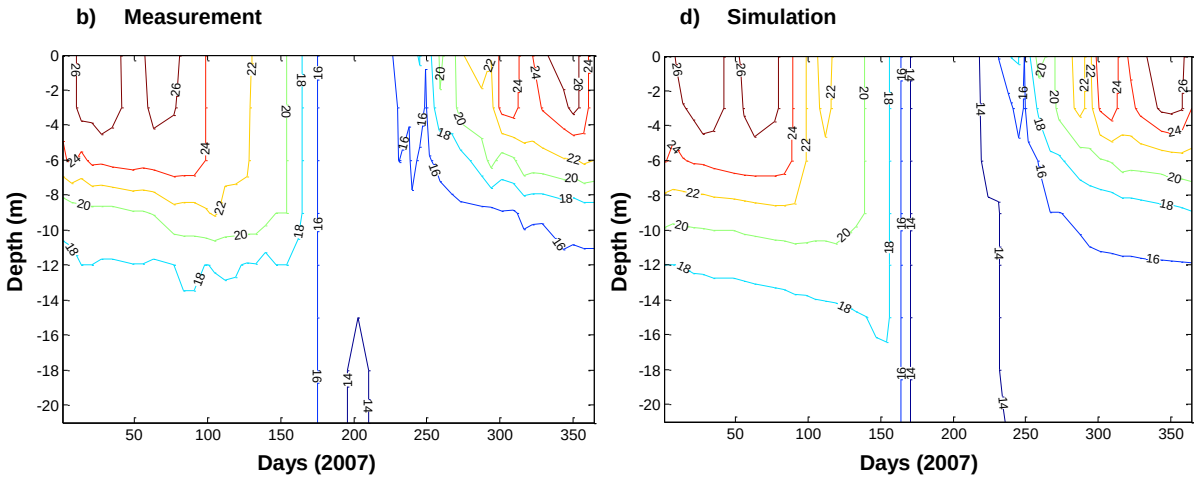

Figure 3. Isotherms for 2007 in Wivenhoe Dam. a) Measured data, b) Simulated data. Available measurements were up to 21 metres under the water

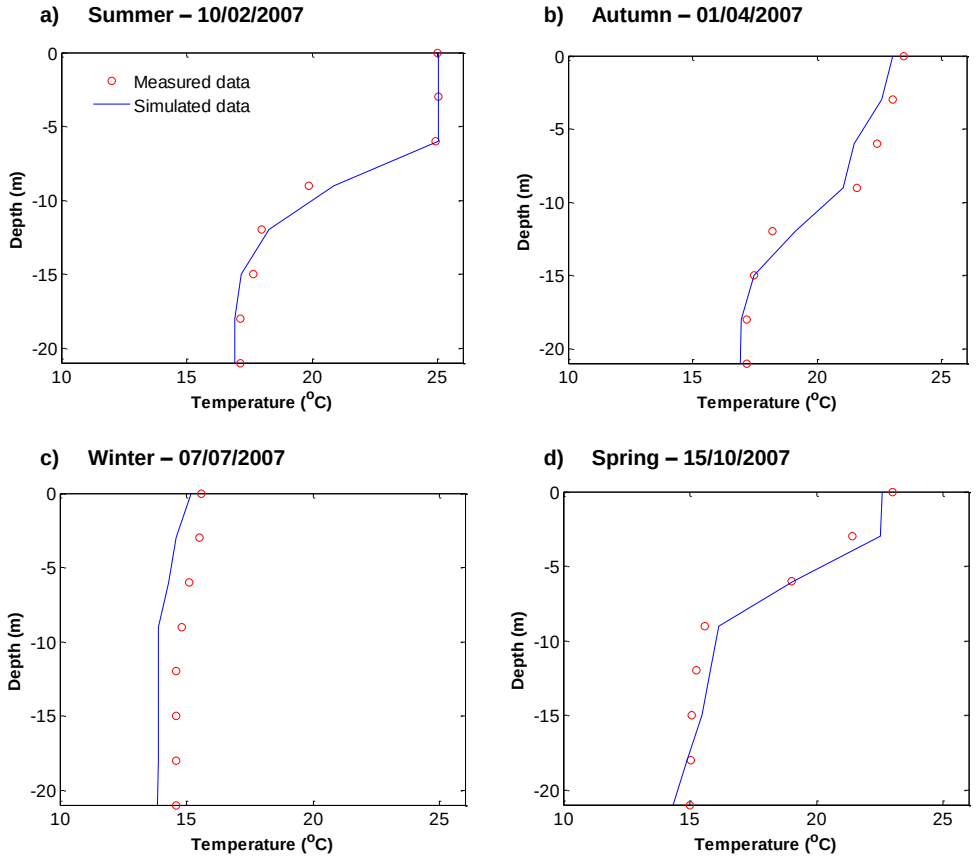

Figure 4. Measured and simulated temperature profiles on four representative days during the simulation period. Solid line = simulated data, red circles = measured data

4.2. Model Verification for Evaporation

DYRESM has been successfully utilised worldwide and validated for the energy balance and water temperature under a wide range of reservoirs and climatic conditions (eg, De Stasio et al., 1996; Schladow and Hamilton, 1997; Gal et al., 2003). This infers that making an exact local validation for evaporation (while ideal) would be not essential. The main reason for this is that DYRESM is a process-based hydrodynamic model with a site-independent hydrodynamic representation (Schladow and Hamilton, 1997).

Hipsey (2006), an important reference for evaporation research, also assumed that the model has been validated for evaporation, given the fact that it relies on parameterisations derived from detailed process studies (both from field and laboratory). This author also states that because of DYRESM's ability to accurately capture in detail the vertical thermal structure, surface water temperature predictions - which are important for evaporation calculation - are predicted to a high level of confidence when compared to other methods. Moreover, for calculation of the flux of latent heat from the water surface to the atmosphere, DYRESM employs the familiar bulk aerodynamic formulae, which have been shown to competently capture the surface fluxes of latent heat, as well as momentum and sensible heat from a variety of water bodies.

In this study, an indirect validation for evaporation was undertaken, based on measurement data collected from a nearby lake. This lake, called Logan's Dam, was chosen because direct measurements of evaporation from Wivenhoe Dam were not made for the study period, nor was there any data available from previous studies so as to perform a site-specific validation. Logan's Dam has a surface area of 17 hectares and a maximum depth of 6.5 m and is located in the same area as Wivenhoe Dam's, approximately 30 km away. Hence, both lakes are under the same generic climatic conditions and, therefore,

evaporation forcing factors are similar. While this in not an ideal validation procedure, it was the best option available, given the lack of appropriate evaporation data for Wivenhoe Dam.

Furthermore, results from other indirect validation methodologies carried out for Wivenhoe Dam will be presented in this section, such as the comparison of DYRESM daily evaporation estimates with evaporation estimates derived from the well-established Penman-Monteith model (Monteith, 1965) and monthly pan evaporation measured by the Australia Bureau of Meteorology (Bureau of Meteorology, 2009a). The latter approach was also used by Hipsey (2006) to show the high accuracy of DYRESM's predictions for evaporation from dams located in different regions in Australia, including Queensland.

Logan's Dam is being used as an experimental site for investigations on evaporation reduction mechanisms (see Helfer et al., 2011b; 2011a; 2010; McJannet et al., 2011) through a project carried out by the Urban Water Security Research Alliance (Urban Water Security Research Alliance, 2010). Helfer et al. (2010; 2011a) used DYRESM to model the water temperature of the lake under baseline and artificial destratification conditions. The model was previously validated for water temperature using daily temperature measurements taken over a 7-month period.

All the water inputs and outputs have been monitored at Logan's Dam so as to accurately determine the evaporation through water balance. From Figure 5, it can be seen that the agreement between the daily evaporation estimated with water balance and the DYRESM estimates are very strong. The coefficient of determination (R^2) is 0.77 with a root-mean-square error (RMSE) of 0.7 mm day^{-1} and a mean bias error (MBE) of 3%.

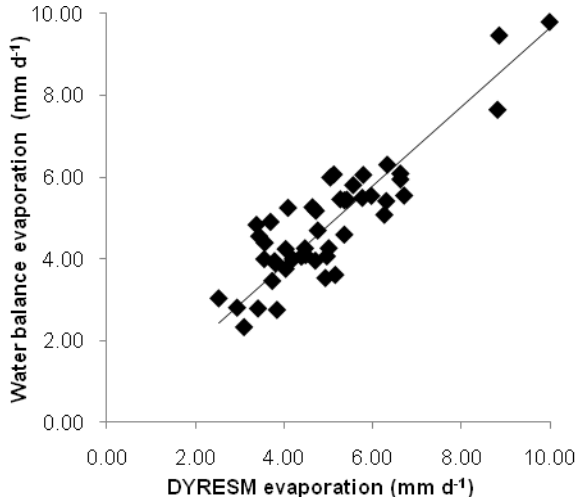

Figure 5. Comparison of DYRESM predicted evaporation and evaporation measured through water balance for Logan's Dam, Queensland

Evaporation rates from Wivenhoe Dam estimated using DYRESM for the year of 2007 (for which reliable water temperature data were available) were compared with evaporation rates estimated using the well-established Penman-Monteith equation, taking into account the heat storage in the water body, as presented by Finch and Hall (2001). We used the temperature data estimated by DYRESM, which compared very well with field data, as shown in the previous section. The simulated temperatures were used rather than measured temperatures because the latter set of data was only available on a weekly basis. For daily evaporation, the agreement between the two models was notable, with a coefficient of determination (R^2) of 0.64, a root-mean-square error (RMSE) of 1.1 mm day^{-1}, and a mean bias error (MBE) of -9.0% for the one-year set of data. The MBE was -6.0% in summer and -1.4% in winter, with the Penman-Monteith estimates being significantly greater than DYRESM's estimates in summer. For monthly estimates, the coefficient of determination was 91%, the RMSE was 0.6 mm day^{-1}, and the MBE was -6.0%.

The 2007-monthly mean daily evaporation estimated with DYRESM was also compared with the 2007-monthly mean daily Class A pan evaporation and with the 18-year monthly mean daily Class A pan evaporation published by the Australian Bureau of Meteorology (BoM).

The pan coefficient used was 0.7, following Stanhill (1976), which is within the published range of values reported for Queensland (Weeks, 1983). The R^2, RMSE and MBE values were 0.84, 0.4 mm day^{-1} and -7.5% respectively, for the 2007 set of data, and 0.70, 0.7 mm day^{-1} and 8.0% for the 18-year monthly average data. The results in Figure 6 show the comparisons of DYRESM estimates for monthly mean daily evaporation with the Penman-Monteith estimates and with the BoM data.

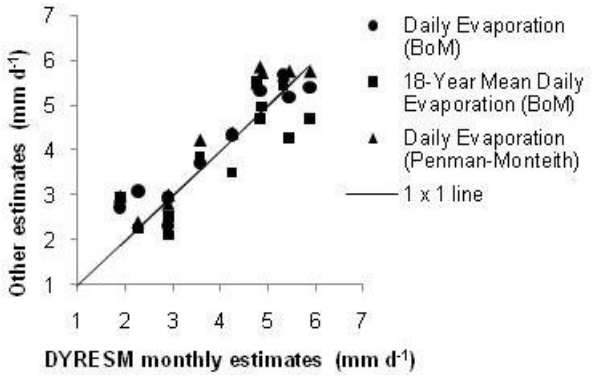

Figure 6. Comparison of DYRESM predicted evaporation and other evaporation estimates

Therefore, in this study, based on the presented indirect validation methods used to evaluate the model DYRESM, we have worked with the assumption that the model has been validated for the calculation of the surface flux of evaporation.

5. Simulations and Discussion

A 3-year period from 01/01/1984 to 31/12/1986 was chosen to study the utilisation of artificial aeration in Wivenhoe Dam. This period was selected due to availability of suitable and consistent data. The measured water temperature profile in January/2007 was used to build an initial profile for January/1984. The very high similarity between the air temperatures in those years was the main reason for this approach. Also, the mean monthly air temperatures in December/2006 and December/1983 were checked against each other. The similarity infers that the previous conditions during both distinct periods would produce similar water profiles in January. In addition, the 2007 data was used to test the sensitivity of the model to the initial profile. The results showed a very low dependence of the temperatures on the

initial profile and depth of the mixed layer, with the temperatures of the first month (January) affected very slightly and temperatures from the end of summer uninfluenced for a wide range of initial temperature magnitudes and depth of the mixed layer.

The initial water level was set at 25 metres, for which the corresponding surface area is 31.2 km^2. The source of the main meteorological data was the SILO database (Bureau of Meteorology, 2009b) which consists of interpolated meteorological variables on a 0.05° (6 km) grid for the whole of Australia (Jeffrey et al., 2001). Wind speed data was taken from the nearest Bureau of Meteorology station, located around 20 km from the study site. Figure 7 shows the meteorological inputs necessary for DYRESM. Mean daily values were used for input.

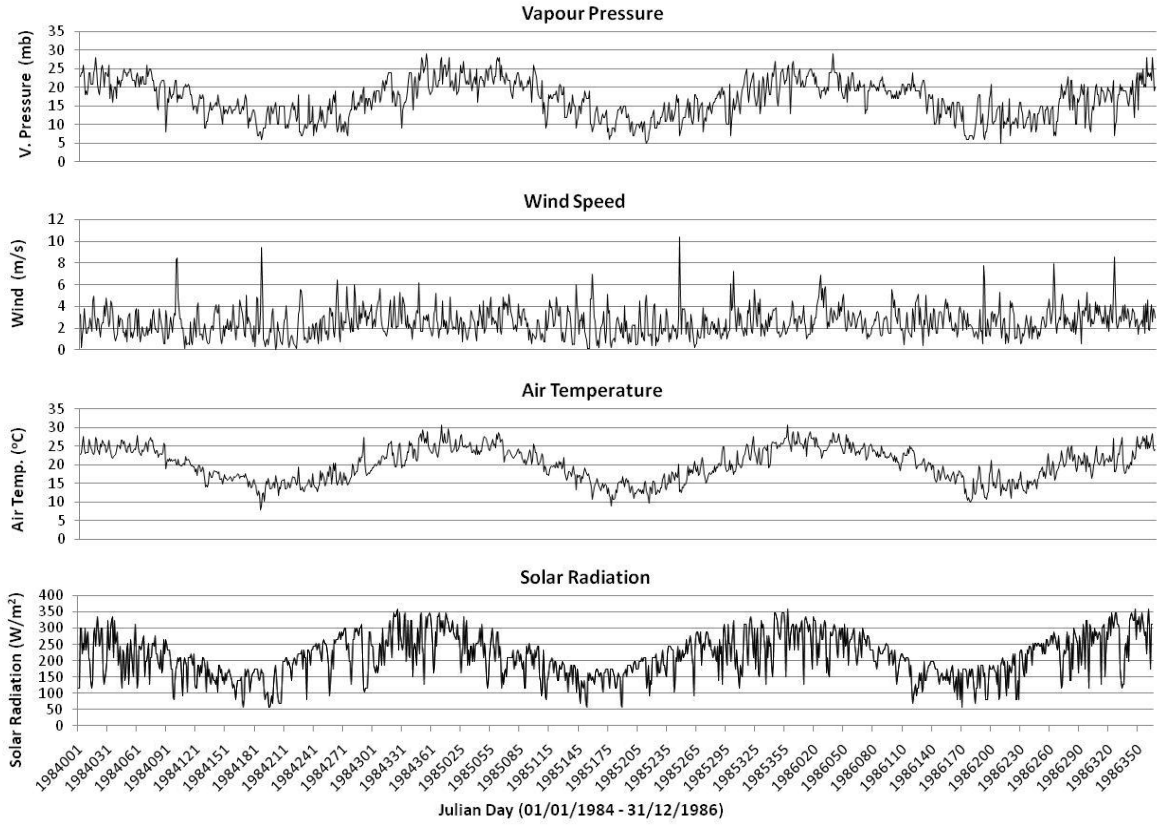

Figure 7. Meteorological data for Wivenhoe Dam. Rainfall, vapour pressure, air temperature and solar radiation are from SILO data drill. Wind Speed was taken from the nearest Bureau of Meteorology station located 20 km from the study site

The Wivenhoe region is characterized by four well-defined seasons, with hot, humid summers and cold, dry winters. The average air temperature in summer during the 3-year period was 25^{o}C and in winter, 14^{o}C. The mean annual temperature was 20^{o}C. These temperatures characterize a typical temperate climate. Solar radiation is also seasonal, with higher values in summer than winter. The average wind speed over the 3-year period was 2.5 m s^{-1} with no distinct seasonal variation. Vapour pressure follows the same trend as temperature and solar radiation, with high values in summer and low values in winter. The deficit of vapour pressure (not shown in the figure) is also higher in summer, indicating that higher rates of evaporation are expected during this season.

5.1. Water Temperature and Evaporation – Baseline simulation

Figure 8 shows the simulated water temperature for the whole period of study. The seasonal variation in temperature is evident, with high temperatures in summer and lower in winter. These are reflection of the seasonal variation of the air temperature and solar radiation shown previously in Figure 7.

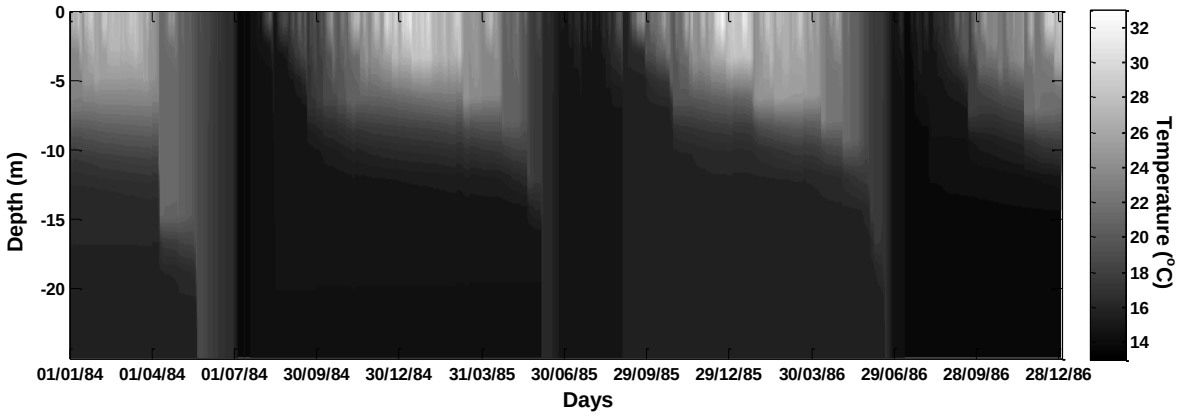

Figure 8. Simulated water temperature for Wivenhoe Dam – 01/01/1984 to 31/12/1986

Thermal stratification persists from September until the beginning of April (the warmer months of the year in Australia), including spring, summer and half of the autumn season. During winter, Wivenhoe is characterised by well-mixed water profiles. The mostly stratified days in the entire period of simulation were 09/02/1984, 11/01/1985, 22/12/1985 and

14/01/1986, with drops of more than 1.5^{o}C m^{-1} in the metalimnion. The average temperature of the hypolimnion during the 3-year period was 15.2^{o}C, varying from 13.8 to 19.3^{o}C. The average surface temperature was 22.5^{o}C, varying from 13.8 to 32.6^{o}C. Table 1 summarises the characteristics of the water temperature and evaporation per season for Wivenhoe Dam, based on this 3-year period simulation.

Table 1. Wivenhoe Dam's baseline water temperature and evaporation for the four seasons – average of 3-year simulated data

	Summer (Dec, Jan, Feb)	Autumn (Mar, Apr, May)	Winter (Jun, Jul, Aug)	Spring (Sep, Oct, Nov)
Surface Temperature (^{o}C)	27.7 (min = 22.1, max = 32.6)	23.6 (min = 17.9, max = 29.5)	16.4 (min = 13.8, max = 20.5)	22.2 (min = 15.9, max = 27.9)
Hypolimnion Temperature (^{o}C)	15.3 (min = 14.2, max = 16.1)	15.6 (min = 14.4, max = 19.2)	15.1 (min = 14, max = 18.5)	14.9 (min = 14.2, max = 16.0)
Depth of well mixed layer (m)[a]	2.5 (min = 0.5, max = 7.0)	7.0 (min = 0.5, max = 25)	17.8 (min = 0.5, max = 25)	3.2 (min = 0.7, max = 25)
Buoyancy frequency (s^{-1})	0.033 (min = 0.025, max = 0.041)	0.025 (min = 0.006, max = 0.037)	0.010 (min = 0.006, max = 0.021)	0.024 (min = 0.006, max = 0.035)
Evaporation (mm/day)	4.6 (min = 0.15, max = 10.9)	3.0 (min = 0.1, max = 11.0)	1.7 (min = 0.1, max = 9.0)	3.6 (min = 0.1, max = 17.2)
Evaporation (mm/season)	412	279	160	323

[a]Depth of well mixed layer is defined as the depth above which the vertical temperature gradient is less than 0.45^{o}C m^{-1}

Figure 9 shows the variation in evaporation rates calculated by DYRESM as a function of the simulated water temperature (Eq. 3 and Eq. 4). Total evaporation is 1,106 mm, 1,140 mm and 1,293 mm for the years of 1984, 1985 and 1986, respectively. The seasonal variation of evaporation is well defined, as a reflection of the air temperatures and solar radiation shown in Figure 7, and also of the water vapour deficit, which is higher in summer and lower in winter. The calculated 3-year average evaporation in summer (December, January and February) is 412 mm, in autumn (March, April and May), 279 mm, in winter (June, July and August), 160 mm and in spring (September, October, November), 323 mm.

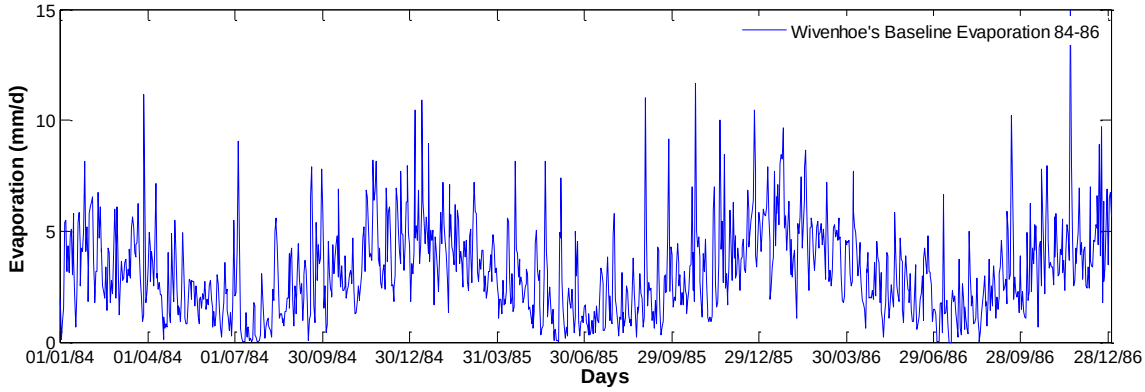

Figure 9. Estimated evaporation from Wivenhoe Dam – 01/01/1984 to 31/12/1986

5.2. Water Temperature and Evaporation under Destratification Conditions

The design of the destratification system to dismantle the thermal stratification of Wivenhoe Dam was based on the model proposed by Asaeda and Imberger (1993), and outlined by Lemckert et al. (1993). The design of the air-flow rate per port is based on the depth of the diffuser in the dam and the stratification strength (buoyancy frequency). The number of ports on each diffuser, in turn, is determined as a function of the reservoir's volume, the designed air-flow rate and the desired time to achieve complete destratification. The model's outputs, therefore, are the air-flow rate to be injected into the water and the number of ports.

For this investigation, the time to achieve complete destratification was set to 5 days. The time was chosen based on the fact that thermal stratification has to be broken rapidly, so that the water at the surface becomes colder from the beginning of the warm season, and higher reductions in evaporation are achieved. For water quality improvement, however, the time usually selected is 21 days (Schladow, 1991; Lemckert et al., 1993).

Based on the simulated water temperature (Figure 8), the diffuser location for the first set of simulations was set at 8 metres above the bottom (approximately 17 metres below the free surface and 7 metres below the stratification zone). This depth was first selected in order to avoid the necessity of pumping high air-flow rates into the water, which would be the case if

the diffuser was placed at the bottom of the lake. It is important to note, however, that the volume of cold water lifted by the 17-m deep destratification system is much less than that lifted by a 25-m deep system and this may be crucial for the effectiveness of the technique. Therefore, a 25-m deep destratification system was also tested in this study.

The stratification profile chosen is from 22/12/1985 (Figure 10), where drops of up to 1.5^{o}C m^{-1} in the metalimnion were observed, with epilimnion temperature equal to 32^{o}C and hypolimnion temperature equal to 14.3^{o}C. The equivalent linear profile N_E (Lemckert and Imberger, 1993) for the 17-m deep destratification system has a magnitude of 0.050 s^{-1}. For the whole water column, N_E = 0.041 s^{-1}.

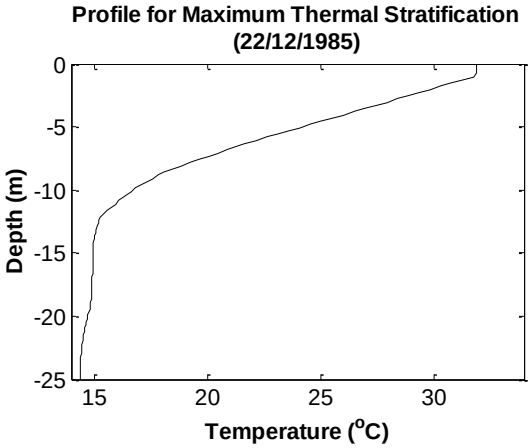

Figure 10. Maximum thermal gradient in Wivenhoe Dam during the period from 01/01/1984 to 31/12/1986

Using the above-mentioned information, the application of the design methodology for the 17-m deep destratification system resulted in 750 plumes, each operating at an air-flow rate of 0.001 m^3 s^{-1}, resulting in a total air-flow rate of 0.75 m^3 s^{-1}. For the 25-m deep system, it resulted in 375 plumes, each operating at an air-flow rate of 0.002 m^3 s^{-1}, totalling 0.75 m^3 s^{-1}**.** The estimated air-flow rate values are relatively high, which can be attributed to the high depth of the dam and to the accentuated thermal gradient.

It can be noted that the second configuration resulted in a higher air-flow rate per plume, which is due to the higher depth of the aerator. The number of plumes, in turn, is related to the volume of the dam, to the net entrainment flow rate per plume (see Lemckert and Imberger, 1993 for definition) and to the time set to have the water destratified. Since the net entrainment flow for the second design (25-m depth) is higher due to a higher air-flow rate, this resulted in a lower number of plumes.

The first set of simulations was performed with the destratification system operating continuously during the entire period of simulation. Afterwards, the simulations were performed with the destratification system operational from the beginning of the stratification season (September) until the end of March. The description of these simulations is presented in Table 2.

Table 2. Summary of the simulated scenarios for Wivenhoe Dam (SIM-1 to SIM-4)

Simulation	SIM-1	SIM-2	SIM-3	SIM-4
Diffuser's depth (below surface)	17 m	25 m	17 m	25 m
Operation	Continuously during the 3-year period	Continuously during the 3-year period	Continuously from September to March each year	Continuously from September to March each year
Air-flow rate per port ($m^3 s^{-1}$)	0.001	0.002	0.001	0.002
Number of ports	750	375	750	375
Total air-flow rate ($m^3 s^{-1}$)	0.75	0.75	0.75	0.75
Parameter M_M	0.13	0.20	0.13	0.20
Parameter C_M	6650	5050	6650	5050
Net entrainment rate ($m^3 s^{-1}$)	472	540	472	540

Each simulation was analysed by assessing: i) the change in evaporation rates, ii) the change in lake temperature (volume-averaged profile temperature, surface temperature and volume-averaged hypolimnetic temperature), iii) the change in the average depth of the mixed layer and iv) the change in buoyancy frequency (an indicator of the mixing efficiency).

All these analyses were done for each season and also for the whole year. The results are shown in Figure 11.

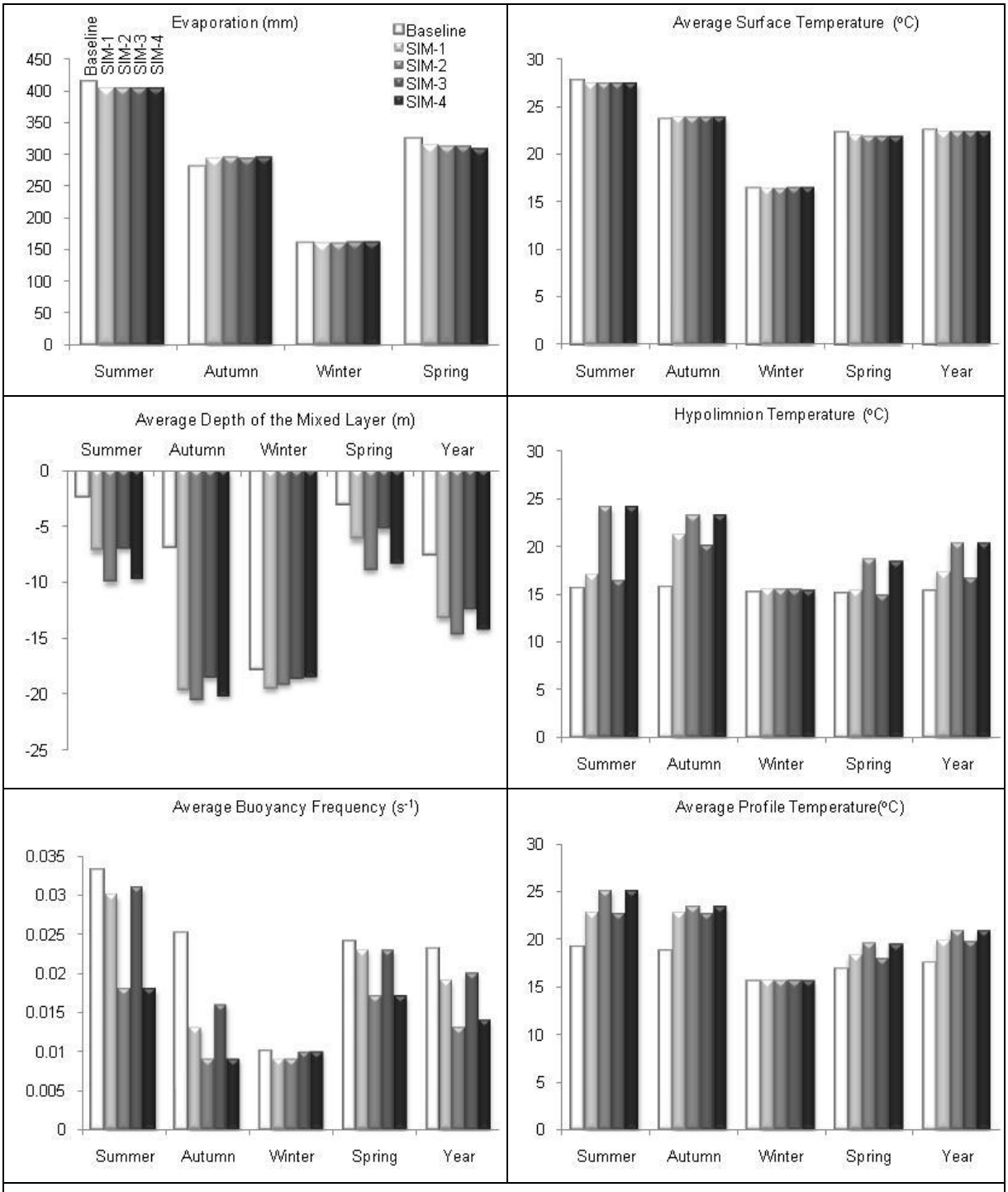

SIM-1: 750 ports, 0.001 $m^3 s^{-1}$, operating continuously during 3 years
SIM-2: 375 ports, 0.002 $m^3 s^{-1}$, operating continuously during 3 years
SIM-3: 750 ports, 0.001 $m^3 s^{-1}$, operating continuously from September to March
SIM-4: 375 ports, 0.002 $m^3 s^{-1}$, operating continuously from September to March

Figure 11. Mean values of lake evaporation, lake temperature, depth of mixed layer and buoyancy frequency for each season – results from the baseline, SIM-1, SIM-2, SIM-3 and SIM-4

The total annual evaporation (average of 3 years) for the baseline scenario resulted in 1179 mm, and the annual evaporation for SIM-1, SIM-2, SIM-3 and SIM-4, was 1173, 1172, 1173 and 1172 mm, respectively, indicating that only minor changes in evaporation rates would be achieved under artificial destratification conditions. There were only slight changes in seasonal evaporation as well. For all simulations, evaporation in summer decreased around 1.7% in relation to the baseline values. In autumn, evaporation increased by around 5.7% for all simulations due to elevation in surface temperature. In winter, evaporation increased by 0.6% for those simulations with no operational destratification system during this season, and no changes were observed for the system operating continuously over the three years of simulation. In spring, all the destratification systems decreased evaporation by around 3.5%. Nevertheless, the net annual saving was only about 0.5%.

As for lake mixing, SIM-2 and SIM-4, with the diffuser placed at the bottom of the lake, were more effective than SIM-1 and SIM-3. This is evidenced by noting the change in the depth of the mixed layer, the average buoyancy frequency, the average water temperature and the bottom temperature as follows. The depth of the mixed layer changed from 7.7 metres in the baseline scenario to around 14.5 metres in SIM-2 and SIM-4. The buoyancy frequency changed from a baseline value of 0.023 s^{-1} to 0.013 s^{-1} in SIM-2 and SIM-4. The buoyancy frequency for SIM-1 and SIM-3 decreased to 0.020 s^{-1}. The simulated water temperatures for SIM-1 and SIM-2 are presented in Figure 12.

The mean lake temperature increased in the aerated-lake scenarios. For SIM-2 and SIM-4, the mean annual temperature increased by 20% and for SIM-1 and SIM-3, by 14%. This indicates that besides increasing mixing, artificial destratification also causes an increase in the heat stored in the water. This is due to the fact that convection is more efficient than diffusion to move heat from the surface, where heating by the sun occurs, to the bottom. This can be corroborated by noting the temperature of the hypolimnion.

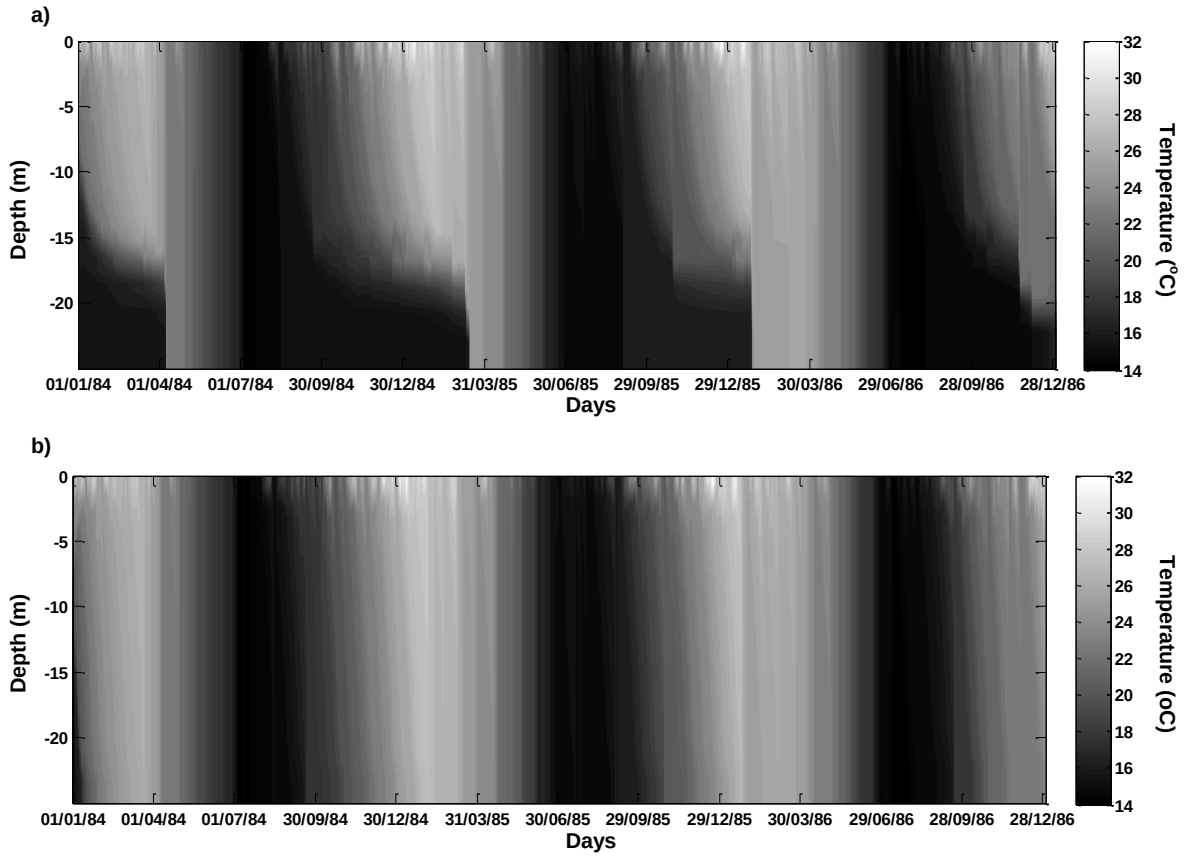

Figure 12. Simulated water temperature for Wivenhoe Dam under destratification conditions for SIM-1 (a) and SIM-2 (b)

The mean annual temperature in the hypolimnion was 15.2^{o}C in the baseline scenario and rose to around 17.0^{o}C in SIM-1 and SIM-3, and to 20.3 ^{o}C in SIM-2 and SIM-4 (the difference is due to the different heights of the destratification system in the water). All these observations indicate that mixing under artificial destratification conditions occurs by the hypolimnion growing at the expense of the epilimnion. In other words, the hypolimnion becomes warmer due to mixing with warmer water from the epilimnion, which is the opposite to the manner in which natural destratification had been observed to occur, with epilimnion cooling at the expense of the hypolimnion. The same conclusion was also reached by Schladow and Fisher (1995).

The temperature profiles on two selected days with high thermal stratification for the baseline scenario and for SIM-4 are compared in Figure 13(a). Although the destratification

system designs used in SIM-1 to SIM-4 were quite effective in mixing the lake for the entire year, the designs were not effective in breaking down the surface stratification for those days with more accentuated temperature gradients (summer). This can be seen from the graph of the 3-year average mixed layer in Figure 11 which shows that artificial destratification increased the average depth of the mixed layer in summer from 2.5 m in the baseline scenario to around 8.0 metres in the scenarios under aeration conditions.

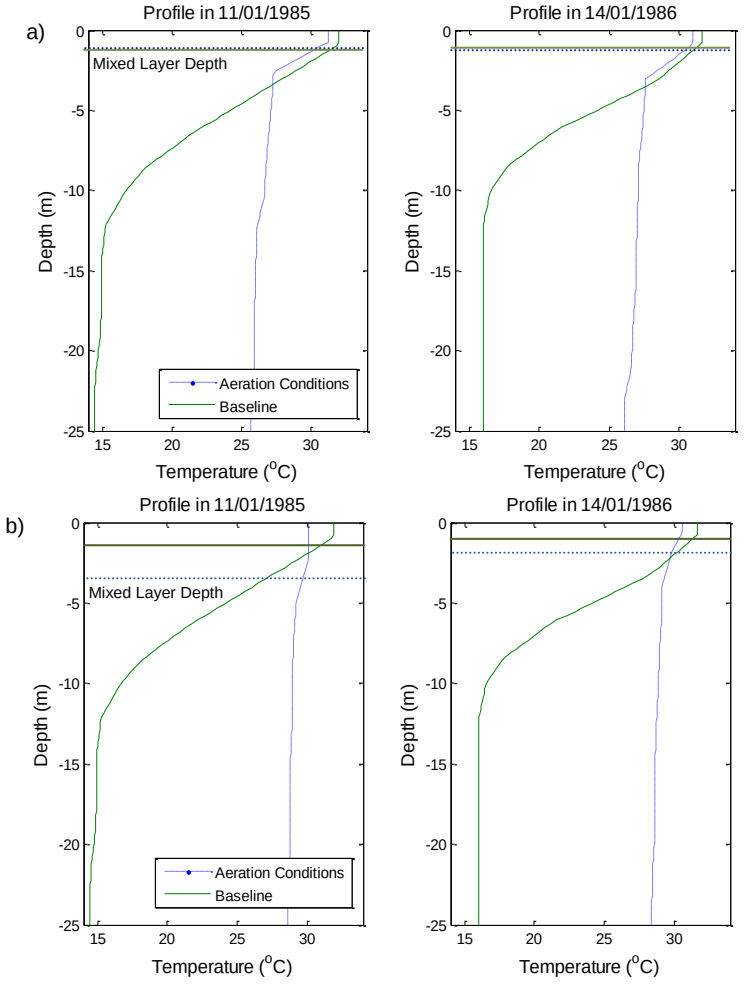

Figure 13. Temperature profiles on two selected days with high thermal gradients and predicted changes under artificial destratification conditions in SIM-4 (a) and SIM-6 (b)

In order to increase the mixing in the reservoir, particularly to lift more cold water to the surface in summer, new destratification designs were set. The idea was to increase the total net entrainment in the lake, which is proportional to the number of plumes. The air-flow rate per plume was kept at 0.002 m^3s^{-1}, following SIM-2 and SIM-4. By doing so, the net

entrainment per plume was also maintained. However, the number of plumes was increased to 750 and then to 1500. The diffuser was considered as being located at the bottom. For both simulations, the destratification system was set to operate from September to March, as the previous simulations showed that artificial destratification is not an efficient mechanism to reduce evaporation from large dams under temperate climates. The new set of simulations is summarized in Table 3.

Table 3. Summary of the simulated scenarios for Wivenhoe Dam (SIM-5 and SIM-6)

Simulation	SIM-5	SIM-6
Diffuser's depth (below surface)	25 m	25 m
Operation	Continuously from September to March each year	Continuously from September to March each year
Air-flow rate per port ($m^3 s^{-1}$)	0.002	0.002
Number of ports	750	1500
Total air-flow rate ($m^3 s^{-1}$)	1.5	3.0
Parameter M_M	0.20	0.20
Parameter C_M	5050	5050
Net entrainment rate ($m^3 s^{-1}$) ($m^3 s^{-1}$)	1080	2160

The profiles of the same days shown in Figure 13(a) are shown in Figure 13(b). The results are from SIM-6. It is evident that the new simulation resulted in a more homogeneous profile than SIM-1, SIM-3 and SIM-4. However, the surface temperature for SIM-6 changed just slightly from the baseline values and the hypolimnion temperature increased significantly, corroborating what was observed from the previous simulations: artificial destratification only contributes to further increasing the heat in the water. Figure 14 shows a summary of the results from SIM-4, SIM-5 and SIM-6, and the baseline.

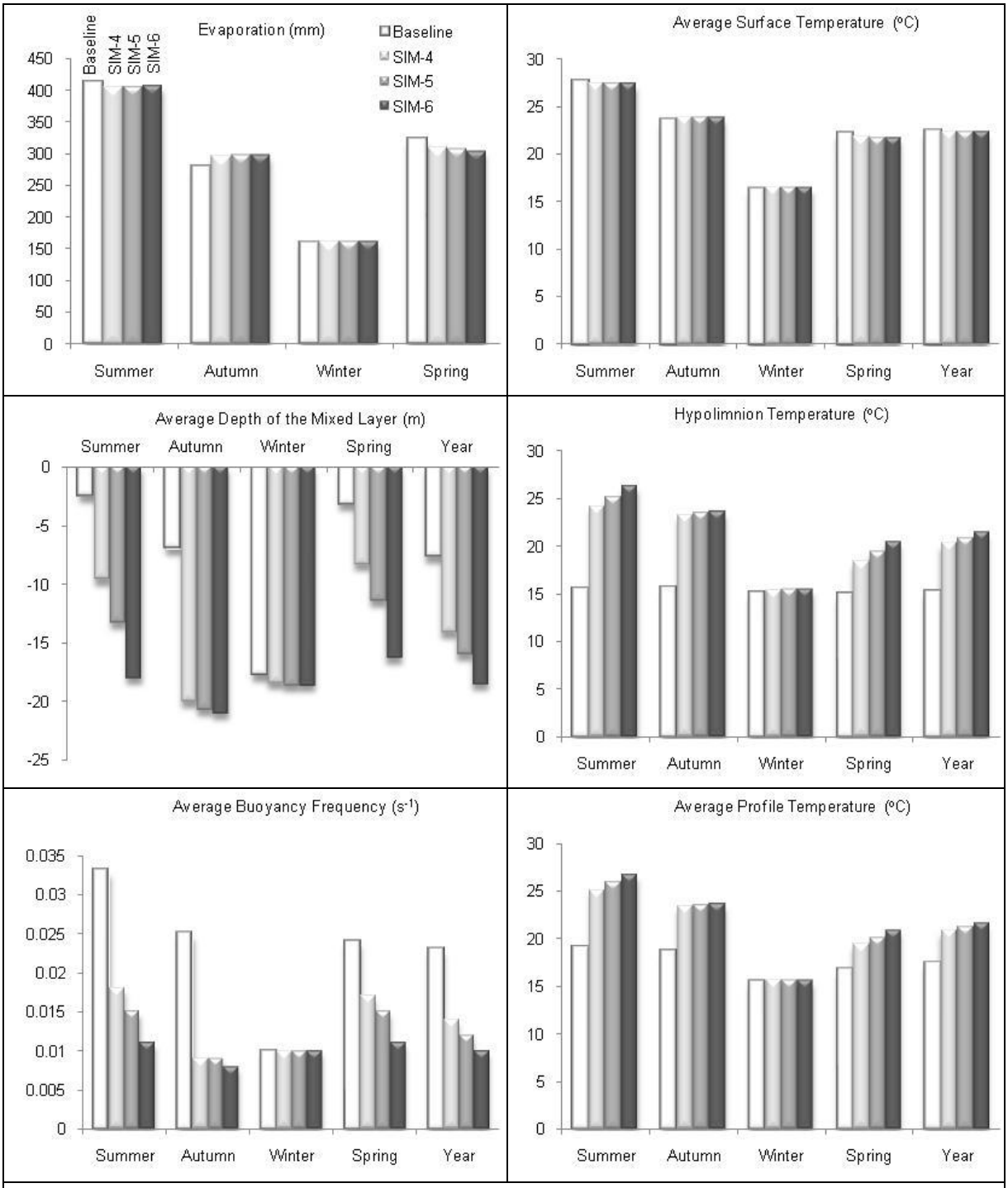

SIM-4: 375 ports, 0.002 $m^3 s^{-1}$, operating continuously from September to March
SIM-5: 750 ports, 0.002 $m^3 s^{-1}$, operating continuously from September to March
SIM-6: 1500 ports, 0.002 $m^3 s^{-1}$, operating continuously from September to March

Figure 14. Mean values of lake evaporation, lake temperature, depth of mixed layer and buoyancy frequency for each season – results from the baseline, SIM-4, SIM-5 and SIM-6

Following the tendencies demonstrated by the first simulations, the new set of simulations also showed that the surface temperature (and evaporation) does not change much when

mixing is increased. Mixing increased from SIM-4 to SIM-6, as evidenced by the diagrams representing the average depth of the mixed layer, the buoyancy frequency, the average profile temperature and the hypolimnion temperature. However, the surface temperature, which is the parameter that directly affects evaporation, remained the same in comparison with the baseline values.

5.3. Seasonal Variation in Temperature and Evaporation Due to Destratification

As the dynamics of the surface water temperature and evaporation did not vary much between the simulations tested in this study, the following analyses for seasonal variation are valid for all simulations presented above.

The effectiveness of air-bubble plume systems in reducing evaporation from Wivenhoe Dam was higher in spring than in any other season. The evaporative reduction in spring in comparison to the baseline evaporation was around 5%. The average temperature was 22.2^{o}C which dropped to 21.9^{o}C after aeration.

The most important reason behind the evaporation reductions in spring was the high drop in surface temperature observed particularly in the beginning of the season, together with the attenuation of the temperature peaks during the whole season. In the beginning of the season, the mild air temperatures and solar radiation did not impart enough heat energy to warm the cold water brought to the surface and a higher reduction in surface temperature, along with evaporation, was observed under destratification conditions. With the continuous operation of the destratification system and the increasing heat added from solar radiation, the temperature of the water in the hypolimnion gradually increased from the beginning to the end of spring. The initial temperature was 14.0^{o}C (September), compared to 22.0^{o}C at the end of November. For the baseline scenario, the expected temperature at the bottom would be 14.0^{o}C from the start to the end of the season. Nevertheless, in the end of spring,

under destratification conditions, the hypolimnion was still slightly colder than the surface. The difference between the two temperatures was around 3.5^{o}C.

In the very beginning of summer, the hypolimnetic water brought to the surface by the destratification system affected surface temperature and reduced evaporation. It was noticed that under destratification conditions, the frequency of surface temperature peaks was reduced in the beginning of summer. On the other hand, the minimum surface temperatures were increased. These indicate that the surface temperature is attenuated under destratification conditions, although the average temperature remains nearly the same. The lower number of days with high temperatures however, led to a slight reduction in evaporation, of 1.7%.

In autumn, evaporation was increased by around 6.0% under destratification conditions, even with the system turned off during this season. This increase is related to the heating that took place during the previous season, when the system was operating. During summer, in the baseline scenario, the average temperature at the bottom was around 15.5^{o}C, while the surface had a much greater temperature, of around 28^{o}C. Under destratification conditions, on the other hand, the temperature at the bottom changed to 25^{o}C, and the surface temperature remained the same (28^{o}C). This shows that the destratification system added more heat to the water, increasing the lake temperature. In the beginning of autumn, the temperature of the water was uniformly warm from top to bottom due to the constant heating and mixing that took place in summer. Under natural conditions, the temperature of the surface would decrease more rapidly during autumn. After destratification took place and the temperature of the lake in the beginning of autumn became warmer, the process of cooling the surface happened more slowly. Therefore, evaporation rates under destratification conditions were slightly higher than the baseline rates in autumn.

In winter, the overturn took place and the water became well mixed and cold from top to bottom, which did not alter evaporation rates.

A new simulation was performed based on the idea that the best solution would be turning on the bubbles for short periods during the warmest season (summer). A continuous operation of the aeration system from September to November (spring) and for 5 successive days in the middle of December, January and February was tested. The results did not differ from the previous ones because the hypolimnion water was warmed up in spring and kept warm during summer bringing no reductions in surface water temperature. A period of cooling down of the hypolimnion would be necessary if the plumes are to be effective in summer.

In order to find a solution, a new simulation was set, this time waiting until summer to turn on the destratification system. The idea was to “save” the cold hypolimnion water until the time when the highest rates of evaporation take place. The aerator was turned on in the beginning of January for only 10 days. When taking a close look at those ten days in January (Figure 15), it was possible to observe that there was a significant reduction in evaporation and surface water temperature during the first seven days of operation of the bubble plume system, the period during which the surface suffered reduction in temperature due to mixing with the cold water from the bottom. After that, the surface temperature started to achieve the same magnitude as the baseline temperature. Eventually, the temperature became higher than the baseline, increasing evaporation. The net reduction in evaporation was therefore, minor. The increase in temperature after turning off the destratification system can be explained by the natural ability of the water column to mix vertically under destratification conditions. This natural mixing, similar to a destratification system, helps introduce more heat to the water, particularly to the surface layer, increasing evaporation.

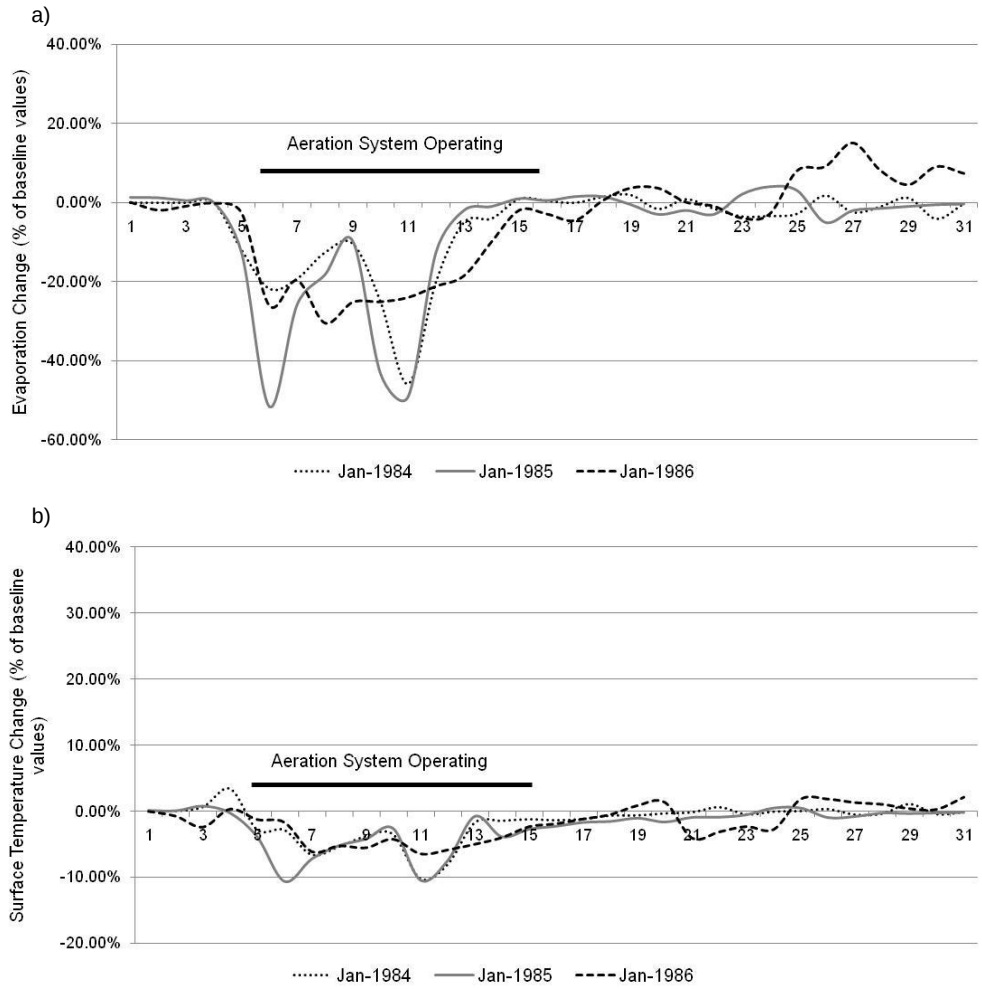

Figure 15. Evaporation (a) and surface temperature (b) changes in January with destratification system operating continuously from 05/01 to 15/01

Figure 16 shows the reduction in evaporation for the 3-year, continuously operating destratification system in comparison with the baseline evaporation. The efficiency of the destratification system in reducing evaporation is significant only in the beginning of the simulation period (January/1984) and decreases in time due to the accumulation of heat within the water column. The January plots show a pronounced increase in evaporation and surface water temperatures in the end of this month, particularly in 1986.

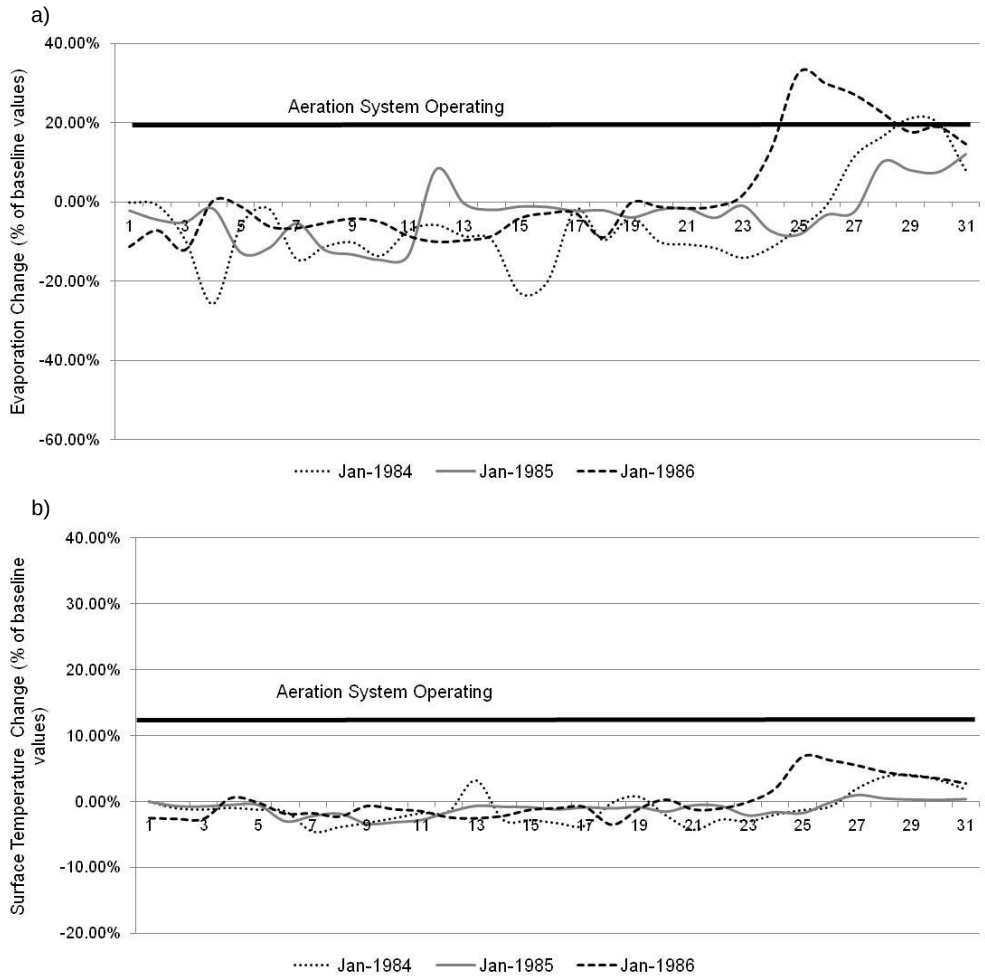

Figure 16. Evaporation (a) and surface temperature (b) changes in January with destratification system operating continuously during the entire month

6. Conclusion

This study investigated the use of destratification by air-bubble plumes as a mechanism to reduce evaporation from large dams. The 1-dimensional model DYRESM was used to model both the natural mixing and the mixing due to artificial aeration and the resultant evaporation rates in Wivenhoe Dam, Australia.

Results from eight different simulations were presented and compared. They consisted of a baseline simulation, in which no destratification system was operated, and 7 simulations in which the lake was under artificial aeration conditions. These conditions varied from a 10-

day operation during periods of higher evaporation rates, to continuous operation of the destratification system over a 3-year period.

From the simulations it was found that none of the operating strategies assessed were efficient in reducing evaporation from Wivenhoe Dam. All simulations decreased evaporation in spring, but this reduction was slight, varying from 2.8 to 4.9% of that expected for a spring without an operational artificial aeration system. In contrast, all of the strategies increased evaporation in autumn. This increase varied from 5.4% to 6.5%, resulting in a net water saving of around 0.6%/year. The influence of the destratification system in winter was insignificant, indicating that it can be turned off during this season.

Apart from the design, the effectiveness of a destratification system in reducing evaporation expectedly depends on the existence of cold temperatures in the hypolimnion associated with warm temperatures in the epilimnion. In temperate lakes, a condition like this would be expected in spring, summer and beginning of autumn. In spring, destratification would be more effective than in summer because the input of heat from solar radiation and heat transfer at the surface is less intense than in summer. In other words, in spring, the time over which the hypolimnion remains colder than the surface (ie, the time until a homogeneous profile is achieved under destratification conditions) is longer. In summer, under destratification conditions this period would be shorter, as the hypolimnetic water brought to the surface would be warmed up quickly due to the constant heat added at the surface and redistributed through the water profile. In this study, for example, the destratification system designed for Wivenhoe Dam was effective in reducing evaporation in January, but after seven days of continuous operation, the heat added at the surface and redistributed through the water profile started to intensify evaporation rates. Using artificial destratification solely in autumn would in turn lead to minor reductions in evaporation rates, because this is the season where evaporation is not as significant as in spring and summer. Finally, aerating the

water in summer and stopping in autumn would leads to high reductions in evaporation at the beginning of the operation of the device followed by a rise in evaporation due to the increase in heat added to the water from the rapid surface heat exchanges, and the net water saving would be minor.

Overall, the results suggest that a continuous source of cold water at the bottom of the lake would make conditions ideal for an artificial destratification system to be effective in reducing surface temperature and evaporation rates, which is unfeasible from the point of view of water management. A possible solution for really deep dams would be moving the diffuser deeper in the water after pre-determined periods of destratification so that the water at the level of the diffuser is always colder than the surface. This would involve increasing the air-flow rate at each dislocation of the aerator to accommodate the change in pressure. This possibility, however, is unlikely to be cost-effective, but still deserves further investigation.

7. Acknowledgements

Funding for this project was provided by Griffith University Postgraduate Research School (GUPRS), Endeavour International Postgraduate Research School (EIPRS), Griffith School of Engineering and the Urban Water Research Security Alliance. The model DYRESM was freely provided by the Centre for Water Research (CWR), the University of Western Australia.

8. References

Amano, K., 2004. Better Application of Destratification Device for Water Quality Improvement in Dam Reservoirs. In: 72nd Annual Meeting of the International Commission on Large Dams, Seoul, May 2004.

Asaeda, T. and Imberger, J., 1993. Structure of Bubble Plumes in Linearly Stratified Environments. J. Fluid Mech., 249, 35-57.

Australian Bureau of Statistics, 2006. Water Account Australia 2004-05. Canberra.

Brutsaert, W., 1982. Evaporation into the Atmosphere: Theory, History and Applications. D. Reidel Publishing Company, Dordrecht, Holland.

Brutsaert, W., 2005. Hydrology: An Introduction. Cambridge University Press, Cambridge, UK, 605 pp.

Bureau of Meteorology, 2009a. Average Annual, Monthly and Seasonal Evaporation. Melbourne, viewed 07 May 2009 <http://www.bom.gov.au/jsp/ncc/climate_averages/evaporation/index.jsp>

Bureau of Meteorology, 2009b. SILO. Bureau of Meteorology.

Burns, F.L. and Powling, I.J., 1981. Destratification of Lakes and Reservoirs to Improve Water Quality. In: Joint United States/Australia Seminar and Workshop, Melbourne, February 19-24.

Cooley, P. and Harris, S.L., 1954. The Prevention of Stratification in Reservoirs. J. Instn. Wat. Engrs., 8, 517-537.

Craig, I. et al., 2005. Controlling Evaporation Loss from Water Storages, National Centre for Engineering in Agriculture Publication 1000580/1, USQ, Toowoomba.

Davis, J.M., 1980. Destratification of Reservoirs - a Design Approach for Perforated-Pipe Compressed-Air Systems. Water Serv., 84, 497-505.

De Stasio, B.T. et al., 1996. Potential Effects of Global Climate Change on Small North-Temperate Lakes: Physics, Fish and Plankton. Limnol. Oceanogr., 41 (5), 1136-1149.

Eichinger, W.E. et al., 2003. Lake Evaporation Estimation in Arid Environments, IIHR Report No. 430, The University of Iowa, Iowa City IA 52242-1585.

Fast, A.W., 1968. Artificial Destratification of El Capitan Reservoir by Aeration. Part I: Effects on Chemical and Physical Parameters. Bulletin 141, Department of Fish and Game, California.

Finch, J.W. and Hall, R.L., 2001. Estimation of Open Water Evaporation, R&D Handbook W6-043/HB for the Environment Agency, UK, 41p.

Fisher, H.B. et al., 1979. Mixing in Inland and Coastal Waters, Academic Press, New York.

Gal, G. et al., 2003. Simulating the Thermal Dynamics of Lake Kinneret. Ecol. Model., 162, 69-86.

Gökbulak, F. and Özhan, S., 2006. Water Loss through Evaporation from Water Surfaces of Lakes and Reservoirs in Turkey. E-Water - electronic journal of the European Water Association (EWA), 2006/7, 1-6. Available on-line < http://www.ewa-online.eu/portale/ewa/ewa.nsf/home?readform >

Helfer, F., Lemckert, C. and Zhang, H., 2011a. Assessing the Effectiveness of Air-Bubble Plume Aeration in Reducing Evaporation from Farm Dams in Australia Using Modelling. In: Water Resources Management Conference 2011, Riverside, May 23-25.

Helfer, F., Lemckert, C. and Zhang, H., 2011b. Investigating Techniques to Reduce Evaporation from Small Reservoirs in Australia. In: 34th IAHR World Congress, Brisbane, Jun 26 – Jul 01. (in press)

Helfer, F., Zhang, H. and Lemckert, C., 2009. Evaporation Reduction by Windbreaks: Overview, Modelling and Efficiency, Technical Report no. 16 for the Urban Water Security Research Alliance, Brisbane.

Helfer, F., Zhang, H. and Lemckert, C., 2010. Evaporation Reduction from Open Storages Using Destratification by Air-Bubble Plumes. In: Riversymposium 2010, Perth, October 11-14.

Henderson-Sellers, B., 1982. Reservoir destratification. In: P.E. Smith (Editor), Techniques and Models in Applying Research to Hydraulic Practice. ASCE, 697–706.

Hicks, B.B., 1972. Some Evaluations of Drag and Bulk Transfer Coefficients over Water Bodies of Different Sizes. Bound.-Lay. Meteorol., 3, 201-213.

Hipsey, M., 2006. Numerical Investigation into the Significance of Night Time Evaporation from Irrigation Farm Dams across Australia. Final Report UWA45, prepared to the Land and Water Resources Research and Development Corporation, Australia.

Hocking, G.C., Sherman, B.S. and Patterson, J.C., 1988. Algorithm for Selective Withdrawal from Stratified Reservoir. J. Hydr. Eng. Div.-ASCE, 114, 707-719.

Hornung, R., 2002. Numerical Modelling of Stratification in Lake Constance with 1-D Hydrodynamic Model DYRESM, Master's thesis, University of Stuttgart, Germany, 101 pp.

Hughes, T.C., Richardson, E.A. and Franckiewicz, J.A., 1975. Evaporation Suppression by Reservoir Destratification, Report prepared to the Water Salvage Potentials in Utah Project, Utah State University, Logan.

Imberger, J. and Patterson, J.C., 1981. A Dynamic Reservoir Simulation Model - DYRESM. In: H.B. Fischer (Editor), Transport Models for Inland and Coastal Waters. Academic Press, New York, 310-361.

Imberger, J. and Patterson, J.C., 1990. Physical Limnology. In: T. Wu (Editor), Advances in Applied Mechanics. Academic Press, Boston, 303-475.

Imberger, J. et al., 1978. Dynamics of Reservoir of Medium Size. J. Hydr. Eng. Div.-ASCE, 104(HY5), 725-743.

Imteaz, M.A., Shanableh, A. and Asaeda, T., 2009. Modelling Multi-Species Algal Bloom in a Lake and Inter-Algal Competitions. Water Sci. Technol., 60(10), 2599-2611.

Imteaz, M.A., Asaeda, T. and Lockington, D., 2003. Modelling the Effects of Inflow Parameters on Lake Water Quality. Environ. Model. Asess., 8(2), 63-70.

Imteaz, M.A. and Asaeda, T., 2000. Artificial Mixing of Lake Water by Bubble Plume and Effects of Bubbling Operations on Algal Bloom. Water Res., 34(6), 1919-1929.

Ivey, G.N. and Patterson, J.C., 1984. A Model of the Vertical Mixing in Lake Erie in Summer. Limnol. Oceanogr., 29, 553-563.

Jeffrey, S.J. et al., 2001. Using Spatial Interpolation to Construct a Comprehensive Archive of Australian Climate Data. Environ. Modell. Softw., 16(4), 309-330.

Kitk, J.T.O., 2003. The Vertical Attenuation of Irradiance as a Function of the Optical Properties of the Water. Limnol. Oceanogr., 48 (1), 9-17.

Kling, G.W., 1988. Comparative Transparency, Depth of Mixing, and Stability of Stratification in Lakes of Cameroon, West Africa. Limnol. Oceanogr., 33(1), 27-40.

Koberg, G.E. and Ford, M.E., 1965. Elimination of Thermal Stratification in Reservoirs and Resulting Benefits. Geol. Surv. Water Supply Pap. 1809-M, Washington DC.

Lemckert, C.J. and Imberger, J., 1993. Energetic Bubble Plumes in Arbitrary Stratification. J. Hydraul. Eng.-ASCE, 119(6), 680-703.

Lemckert, C.J., Schladow, S.G. and Imberger, J., 1993. Destratification: Some Rational Design Rules. In: Australian Water and Wastewater Association 15th Federal Convention, Gold Coast, April 18-23.

Lewis, D.M. et al., 2001. Numerical Simulation of Surface Mixers Used for Destratification of Reservoirs. In: MODSIM'2001 International Congress on Modelling and Simulation, Perth, December 10-13, p. 311-316.

Lorenzen, M.W. and Fast, A.W., 1977. A Guide to Aeration/Circulation Techniques for Lake Management, EPA-600/3-77-004, Ecological Res. Services/Envir. Protection Agency, Washington DC.

Martínez Alvarez, V. et al. 2008. Regional Assessment of Evaporation from Agricultural Irrigation Reservoirs in a Semiarid Climate. Agr. Water Manage., 95, 1056-1066.

McDougall, T.J., 1978. Bubble Plumes in Stratified Environments. J. Fluid Mech., 85, 655-672.

McJannet, D. et al., 2011. Estimation of Evaporation and Sensible Heat Flux from Open Water Using a Large Aperture Scintillometer. Water Resour. Res. (in press)

McJannet, D., Cook, F. and Burn, S., 2008a. Evaporation Reduction by Manipulation of Surface Area to Volume Ratios: Overview, Analysis and Effectiveness, Technical Report 8 for the Urban Water Security Research Alliance, Brisbane.

McJannet, D. et al., 2008b. Evaporation Reduction by Monolayers: Overview, Modelling and Effectiveness, Technical Report 6 for the Urban Water Security Research Alliance, Brisbane.

Milgram, J.H., 1983. Mean Flow in Round Bubble Plume. J. Fluid Mech., 133, 345-376.

Monteith, J.L., 1965. Evaporation and the Environment. In: G.E. Fogg (Editor), The State and Movement of Water in Living Organisms. Academic Press, New York, 205-234.

Mortimer, C.H., 1941. The Exchange of Dissolved Substances Between Mud and Water in Lakes. Part 1 and 2. J. Ecol., 29, 147-201.

National Land & Water Resources Audit, 2001. Australian Water Resources Assessment 2000. Canberra.

Oliver, R.L. et al., 2000. The Darling River: Algal Growth and the Cycling and Sources of Nutrients, Murray Darling Basin Commission, Project M386, Final Report.

Patterson, J.C., Hamblin, P.F. and Imberger, J., 1984. Classification and Dynamic Simulation of the Vertical Density Structure of Lakes. Limnol. Oceanogr., 29(4), 845-861.

Patterson, J.C. and Imberger, J., 1989. Simulation of Bubble Plume Destratification Systems in Reservoirs. Aquat. Sci., 51(1), 3-18.

Penman, H.L., 1948. Natural Evaporation from Open Water, Bare Soil and Grass. Proceedings of the Royal Society. London A193, 120-146.

Rosenberry, D.O. et al., 2007. Comparison of 15 Evaporation Methods Applied to a Small Mountain Lake in the Northeastern USA. J. Hydrol., 340(3-4), 149-166.

Schladow, S.G., 1991. A Design Methodology for Bubble Plume Destratification Systems. In: International Symposium on Environmental Hydraulics Hong Kong, December, pp. 173-178.

Schladow, S.G., 1992. Bubble Plume Dynamics in a Stratified Medium and the Implications for Water Quality Amelioration in Lakes. Water Resour. Res, 28(2), 313-321.

Schladow, S.G., 1993. Lake Destratification by Bubble-Plume Systems: Design Methodology. J. Hydraul. Eng.-ASCE, 119(3), 350-368.

Schladow, S.G. and Fisher, I.H., 1995. The Physical Response of Temperate Lakes to Artificial Destratification. Limnol. Oceanogr., 40(2), 359-373.

Schladow, S. and Hamilton, D., 1997. Prediction of Water Quality in Lakes and Reservoirs. Part 2 - Model Calibration, Sensitivity Analysis and Application. Ecol. Model., 96, 111-123.

Scott, W. and Foley, A.L., 1921. A Method of Direct Aeration of Stored Waters. Proc. Ind. Acad. Sci., 1919, 71-73.

Seqwater, 2009. Wivenhoe Dam. Seqwater, Brisbane, viewed 01 July 2010 < http://www.seqwater.com.au/public/source-store-treat-supply/dams/wivenhoe-dam >

Spigel, R.H. and Imberger, J., 1980. The Classification of Mixed-Layer Dynamics in Lakes of Small to Medium Size. J. Phys. Oceanogr., 10(7), 1104-1121.

Stanhill, G., 1976. The CIMO International Evaporimeter Comparison. Publication 449 of the World Meteorological Organization, Geneva, 38 p.

Tanentzap, A.J., 2006. Applying a Numerical Model to Determine whether Long-Term Changes in Dissolved Organic Carbon and Wind Speed Increase Cold-Water Habitat in a Canadian Shield Lake. Technical Report for the Cooperative Freshwater Ecology Unit, Laurentian University, Sudbury, Ontario, 74 p.

Tanentzap, A.J., Hamilton, D.P. and Yan, N.D., 2007. Calibrating the Dynamic Reservoir Simulation Model (DYRESM) and Filling Required Data Gaps for One-Dimensional Thermal Profile Predictions in a Boreal Lake. Limnol. Oceanogr.: Methods, 5, 484-494.

Tennessee Valley Authority. 1972. Heat and Mass Transfer between a Water Surface and the Atmosphere, Water Resources Research Laboratory Report No 14 prepared for the Tennessee Valley Authority, Report No. 0-6803.

Tolland, H.G., 1977. Destratification/Aeration in Reservoirs, Technical report TR 50, Water Research Centre, England.

Urban Water Security Research Alliance, 2010. Water Loss Reduction, Brisbane, viewed 11 Jan 2011 < http://www.urbanwateralliance.org.au/projects/project9.html >

van Dijk, M. and van Vuuren, S.J., 2009. Destratification Induced by Bubble Plumes as a Means to Reduce Evaporation from Open Impoundments. In: 2008 Water Institute of Southern Africa Biennial Conference, Sun City, South Africa, May 18-22, 2008.

Weeks, W.D., 1983. The Calculation of Evaporation in Queensland. Queensland Division Technical Paper, v. 24, no. 4, Institution of Engineers, Brisbane.

Yao, X., 2008. An Improved 2-D Numeric Model for Open-Water Daily Evaporation Estimation, Bachelor's thesis, Griffith University, Australia, 59 pp.

Yao, X. et al., 2010. Evaporation Reduction by Suspended and Floating Covers: Overview, Modelling and Efficiency, Technical Report no. 28 for the Urban Water Security Research Alliance, Brisbane.

Yeates, P.S. and Imberger, J., 2003. Pseudo Two-Dimensional Simulations of Internal and Boundary Fluxes in Stratified Lakes and Reservoirs. International Journal of River Basin Management, 1(4), 297-319.